An exact approach for the multi-depot electric vehicle scheduling problem

Xenia Haslinger[a]   Elisabeth Gaar[b]

Sophie N. Parragh[a]

[a] Johannes Kepler University Linz, Institute of Production and Logistics Management,

JKU Business School, Altenberger Straße 69, 4040 Linz, Austria

[b] University of Augsburg, Institute of Mathematics,

Universitätsstraße 14, 86159 Augsburg, Germany

Abstract

The "avoid - shift - improve" framework and the European Clean Vehicles Directive set the path for improving the efficiency and ultimately decarbonizing the transport sector. While electric buses have already been adopted in several cities, regional bus lines may pose additional challenges due to the potentially longer distances they have to travel.

In this work, we model and solve the electric bus scheduling problem, lexicographically minimizing the size of the bus fleet, the number of charging stops, and the total energy consumed, to provide decision support for bus operators planning to replace their diesel-powered fleet with zero emission vehicles. We propose a graph representation which allows partial charging without explicitly relying on time variables and derive 3-index and 2-index mixed-integer linear programming formulations for the multi-depot electric vehicle scheduling problem. While the 3-index model can be solved by an off-the-shelf solver directly, the 2-index model relies on an exponential number of constraints to ensure the correct depot pairing. These are separated in a cutting plane fashion.

We propose a set of instances with up to 80 service trips to compare the two approaches, showing that, with a small number of depots, the compact 3-index model performs very well. However, as the number of depots increases the developed branch-and-cut algorithm proves to be of value. These findings not only offer algorithmic insights but the developed approaches also provide actionable guidance for transit agencies and operators, allowing to quantify trade-offs between fleet size, energy efficiency, and infrastructure needs under realistic operational conditions.

1   Introduction

CO_2-emissions from transport accounted for about 21% of the global CO_2-emissions in 2023, increasing by almost 80% between 1990 and 2023 (Statista, 2024a,b). Following the "avoid - shift - improve" framework to meet the Paris Climate Agreement, Austria's 2030 Mobility Masterplan promotes active modes of transport, like walking and biking, public modes of transport, and shared mobility as well as decarbonizing the transportation sector in general (BMK, 2021). The

implementation of the European Clean Vehicles Directive (EU, 2019) requires all member states to meet at least half of their procurement targets for clean buses via zero emission buses. E.g., Austria's target for heavy duty vehicles (including buses) is currently 45% and will rise to 65% with January 2026. The Austrian research project "Zero Emission Mobility Salzburg" (ZEMoS) is a collaborative effort of several public and private institutions and research organizations to support the transition from diesel-powered to zero emission public bus transport and waste collection vehicles. The main focus is the decarbonization of the regional public bus system (ZEMoS, 2023; Peters et al., 2024; Haslinger et al., 2023).

In order to support the transformation of the public bus system in European countries and beyond, high-quality decision support is necessary, especially, concerning the bus operators' important strategic decision of how many and which types of zero emission buses to invest in. Given an available line plan, switching from diesel-powered buses to zero emission vehicles without changes in the plan, requires solving an (electric) vehicle scheduling problem, minimizing the number of buses required to serve the line. Since battery-electric zero emission vehicles are currently still only available with rather limited driving ranges compared to diesel-powered vehicles, and have the disadvantage of taking a long time to recharge, it is not straightforward to substitute conventional diesel buses with zero emission technology, in particular for regional bus lines. Commercial transport, especially the schedule-based sector, operates with a high level of planning to ensure schedules are performed with high punctuality according to the timetable. Effectively integrating electric buses into these systems requires careful consideration of their operational constraints (Wen et al., 2016). Recharging stops during the day are usually required and have to be planned. From an operator's perspective, charging on their own premises, potentially relying on their own photovoltaic energy, is in many cases the cheapest and sometimes the only option, since chargers for heavy duty vehicles are not yet available on a larger scale, resulting in a rather small number of possible charging locations.

The problem we address can be cast as a Multi-Depot Electric Vehicle Scheduling Problem (MDEVSP): each bus line operator has to serve a set of service trips with a fleet of electric or fuel cell-electric vehicles. Each service trip has to be covered by exactly one schedule, which is performed by one vehicle. Each vehicle is required to begin and end its trip at the same depot, chosen from a predefined set of depots. Given the use of electric vehicles and the regional setting with relatively long bus routes, charging may need to be planned throughout the day to ensure that the battery level never drops below a specified threshold and remains above a certain limit upon returning to the depot. Recharging requires vehicles to drive to a charging station, where charging facilities are usually available. Partial recharging is allowed.

The aim of our approach is to provide decision support for transitioning from diesel-powered to zero emission vehicles, particularly electric buses. The key issue to resolve is determining how many buses are necessary to serve all service trips. Service trips follow a timetable and, therefore, they have fixed start and end times, durations, and lengths. We also assume that the fleet is limited to a single vehicle type, i.e., buses of a specific length and technology. This reflects the situation currently encountered in Salzburg, where individual lines are tendered and assigned to different operators based on their bids. However, various bus types can be evaluated

and compared to select the most suitable option. Since minimizing the total number of vehicles usually results in several alternative optimal solutions, we lexicographically minimize (1) the number of vehicles, (2) the number of charging events during the day, and (3) the total energy consumed, while all scheduled service trips during daily operations are covered.

The contribution of this paper is as follows:

- We develop a graph representation that only allows time-feasible paths (or vehicle schedules), including charging events.

- We formulate a 3-index and a 2-index mixed-integer linear program (MILP), relying on our graph representation, allowing partial recharge without explicitly modeling time.

- The 3-index model is compact and can be solved directly with an off-the-shelf solver. The 2-index model requires depot-pairing constraints of exponential size. We propose two different ways to model these constraints (infeasible path constraints and connectivity constraints) and separate them in a branch-and-cut fashion.

- We present a computational study on a large set of instances that mimic realistic settings and illustrate the advantages and drawbacks of the two approaches.

The remainder of this paper is structured as follows. We first give an overview of the work related to the problem setting considered in this paper in Section 2. We then formally define the MDEVSP with partial recharging and detail a graph representation of it in Section 3. Next, we present two mathematical formulations for the MDEVSP, one with three and one with two indices in Section 4. We propose a branch-and-cut algorithm to solve this problem in Section 5. The algorithm is tested on newly generated MDEVSP benchmark instances based on instances from the literature. Computational results are provided in Section 6, followed by the conclusions in Section 7.

2 Literature review

Electric vehicle scheduling problems have attracted quite some attention over the past years. In the following, we review some of the most closely related contributions, starting with the work of Li (2014) who studied the single-depot electric vehicle scheduling problem (EVSP) without partial charging, and have shown that it is NP-hard. They develop a branch-and-price approach, considering battery swapping or fast charging up to battery capacity in conjunction with maximum distance constraints.

Wen et al. (2016) present a MILP for the MDEVSP considering partial charging relying on an almost acyclic network representation but requiring time variables, minimizing a combination of travel and vehicle costs. Larger instances are addressed by a large neighborhood search algorithm.

Wang et al. (2021) develop a column generation algorithm and combine it with a genetic algorithm to address the MDEVSP of three bus lines in Qingdao, China. Adler and Mirchandani (2017) address the the MDEVSP with partial recharge, minimizing the total schedule costs,

limiting the number of buses, which can be stationed at each depot. A branch-and-price algorithm is developed and used to benchmark a heuristic approach on random instances with up to 50 service trips. The heuristic is then applied to a large-scale data set from the metropolitan area of Phoenix. Janovec and Koháni (2019) develop a MILP for the single-depot problem with electric vehicles, considering possible charging events at each of the available chargers. Their formulation requires 4-index variables and, similar to our approach, they do not rely on time variables explicitly. The model is applied to case study-based data and solved by Xpress IVE. Up to 160 service trips are considered.

Hu et al. (2022) address the optimization of locating fast chargers, which allow en-route charging at selected bus stops along three bus routes in Sydney, and determining charging schedules assuming time-dependent electricity prices. They also consider the possibility to delay service, but penalize passenger waiting times. Passenger demand as well as travel times are assumed to be uncertain. The developed robust optimization model is solved by Gurobi. Time-of-use electricity prices are also considered by van Kooten Niekerk et al. (2017), Li et al. (2020), and Wu et al. (2022) in a deterministic setting. van Kooten Niekerk et al. (2017) present two mathematical programming models for the single-depot case, where in the first, a linear charging process with constant electricity prices during the day is assumed. The second model allows any type of charging process, includes time-of-use electricity prices, and takes the depreciation cost of the battery into account. For the latter model, the exact value charged is approximated by discretizing it. Instances with up to 175 service trips are solved to optimality with both models, for larger instances with 241 service trips, methods based on column generation are deployed. Wu et al. (2022) formulate the problem with two objectives, which are considered in a lexicographic fashion and develop a branch-and-price algorithm. Also Liu and Ceder (2020) address the combined problem of vehicle scheduling and charger location, allowing partial recharge for transit buses in Shanghai. The developed modeling approaches rely on deficit function theory and mixed-integer programming. The location of charging infrastructure in combination with electric bus scheduling and a single depot is modeled as a 2-index MILP by Stumpe (2024) and, using Gurobi as the solver engine, applied to large-scale instances. Zhou et al. (2024) propose a MILP and a set-covering formulation for the electric bus charging scheduling problem with a mixed fleet of electric vehicles, partial recharging while taking battery degradation effects into account. A branch-and-price algorithm solves instances with up to 100 service trips, for tackling large-scale instances, an optimization-based adaptive large neighborhood search (ALNS) is developed.

A mixed fleet of conventional and electric vehicles is also considered by Sassi and Oulamara (2017). Since charging costs change over time, in the developed model, time is discretized and costs are minimized in the objective function. Also, maximum grid capacity constraints are considered. Rinaldi et al. (2020) address mixed fleet bus scheduling with a single depot. Time is discretized, assuming that buses can be fully charged within one time interval. Trip departure times may deviate from their preferred time. The developed MILP is decomposed into smaller subproblems and applied to case study data from Luxembourg City. Yıldırım and Yıldız (2021) also address a mixed fleet problem, but with multiple depots and with multiple

4

different charging technologies and develop an efficient column generation-based algorithm to determine the minimum cost fleet configuration for large-scale real-world instances. Zhang et al. (2022) present a mixed-integer programming formulation for the MDEVSP with heterogeneous vehicles. They solve the model using CPLEX and propose an ALNS algorithm to address the problem, incorporating a partial mixed-route strategy and a partial recharging policy. Frieß and Pferschy (2024) have developed a MILP, where different zero emission propulsion technologies are considered concurrently to optimize the bus fleet mix for serving the city of Graz, Austria. In order to solve the model, they pre-select a set of possible options for buses to switch between different lines.

Zhang et al. (2021) address electric bus fleet scheduling with a single depot, non-linear charging and battery fading, and develop a branch-and-price approach. Non-linear charging, considering battery degradation effects are also studied by Zhou et al. (2022). A column-generation based heuristic enhanced by ideas from machine learning has recently been developed by Gerbaux et al. (2025) and applied to the MDEVSP with non-linear charging. Also Diefenbach et al. (2022) consider non-linear charging in an in-plant vehicle scheduling application of the multi-depot problem. In their case, vehicles are free to return to any depot, not necessarily the one they started from. They address this problem setting by a branch-and-check approach, moving all complicating aspects, such as the planning of charging events, to the subproblem and generate cutting planes, enforcing a change in the current solution, when violated. Löbel et al. (2024) propose a MILP for the electric bus scheduling problem with a single depot for mixed fleets of electric and non-electric vehicles, presenting an improved approximation of non-linear battery charging behavior of the electric vehicles. Furthermore, they address the challenge of adjusting to power grid bottlenecks by integrating dynamic recharging rates and time-of-use electricity prices. Partial charging is allowed and available charging slots must not be exceeded. The model is applied on diverse real-life instances with up to 1,207 service trips.

Capacitated charging stations in conjunction with partial recharging in the context of electric vehicle scheduling in public transit is considered by de Vos et al. (2024). They rely on a path-based formulation which is solved by column generation. Integer solutions are obtained by price-and-branch and a diving heuristic. Instances with up to 816 service trips are addressed.

Jiang and Zhang (2022) present a mixed-integer program and develop a branch-and-price algorithm to address real-world instances of the MDEVSP with up to 460 service trips, considering a partial recharging policy, time windows for service trip start times, and charging depots located in close proximity to the start and end stops of each line. The proposed branch-and-price algorithm is improved by incorporating a heuristic approach to generate good initial solutions as well as by embedding heuristic decision-making within the label-setting algorithm to solve the pricing problem. Also the branching step is enhanced by heuristic rules for fixing variables to 0 or 1, if their fractional values are very close to these values. Single line instances without time windows and up to 200 service trips are solved to proven optimality.

Gkiotsalitis et al. (2023) propose a mixed-integer non-linear model, which they later reformulate to a MILP, for the electric MDVSP with time windows, where operational cost of buses as well as vehicle waiting time are considered and service trips may start within a certain time

window. In their formulation, simultaneously charging different vehicles on the same charger is prohibited. The authors introduce valid inequalities to tighten the search space of the MILP. The implementation is demonstrated on a toy network and on randomly generated benchmark instances similar to Carpaneto et al. (1989). For further work on electric bus scheduling we refer to the survey conducted by Perumal et al. (2022).

3   Graph representation of the MDEVSP

On the way to our ultimate goal of solving the MDEVSP by utilizing mixed-integer linear programming, we first lay the foundations in this section. In particular, we formally introduce the MDEVSP in Section 3.1, and then we detail in Section 3.2 how any instance of the MDEVSP can be transformed into a graph, such that solving a particular kind of flow problem in this graph is equivalent to solving the MDEVSP for this instance.

3.1   Description of the MDEVSP

We start by giving the formal definition of the MDEVSP. In the MDEVSP, we are given a set of timetabled service trips V^I, where each service trip $i \in V^I$ corresponds to a scheduled trip with a specific start time s_i and end time e_i, a duration u_i and an energy usage q_i. Moreover, each service trip i has a start location ℓ_i^s and an end location ℓ_i^e.

Furthermore, we are given the set of depot indices K and for each depot index $k \in K$ we are given the number of available vehicles b_k and the depot location ℓ_k. Note that the depots for different depot indices can be at the same physical location. For notational convenience we introduce the set of origin depots O consisting of o_k for all $k \in K$, and the set of destination depots D consisting of d_k for all $k \in K$. For each depot index $k \in K$, we define the start and the end location of the origin and destination depot as ℓ_k, so $\ell_{o_k}^s = \ell_{o_k}^e = \ell_{d_k}^s = \ell_{d_k}^e = \ell_k$ hold.

Moreover, we are given the set of charging stations C, where each charging station $a \in C$ has a location ℓ_a, which serves as both start and end location, so $\ell_a^s = \ell_a^e = \ell_a$. The locations of the charging stations can be at any specified physical location and may coincide with the depot locations.

For each pair of service trips, origin or destination depots, or charging stations $i, j \in V^I \cup O \cup D \cup C$, we are given the traveling time from ℓ_i^e to ℓ_j^s (i.e., the time it takes a vehicle to travel from the end location of i to the start location of j) as t_{ij}, and the distance between ℓ_i^e and ℓ_j^s as d_{ij}. Moreover, we compute the energy usage p_{ij} between the locations ℓ_i^e and ℓ_j^s as $p_{ij} = \theta d_{ij}$, where θ is the given energy consumption rate, i.e., the amount of energy used per distance unit. Thus, a vehicle's energy consumption is assumed to be a linear function of the traveled distance.

Furthermore, the maximum battery capacity of the electric vehicles s^{max}, the minimum allowed battery level s^{min}, the minimum allowed battery level when returning to the depot at the end of the schedule s_{dep}^{min} (with $s_{dep}^{min} \geq s^{min}$), the minimum time that needs to be available for charging t^{min} and the charging rate r, i.e., the time needed to charge one unit of the battery, are given. From that we can compute the time required to fully charge the battery t^{max} as

$t^{max} = \frac{1}{r}(s^{max} - s^{min})$. A vehicle's charging time is assumed to be a linear function of the amount that its battery is charged.

The goal of the MDEVSP is to find a schedule, such that (1) each timetabled service trip $i \in V^I$ is done by exactly one vehicle, (2) each vehicle starts in some depot $k \in K$, performs a sequence of service trips and returns to the same depot k at the end of the day, (3) between two service trips or between a service trip and returning to the depot, each vehicle visiting a charging station can reload its battery for at least t^{min} minutes with charging rate r, (4) each vehicle starts at its depot with energy level s^{max} and returns to its depot with energy level at least s_{dep}^{min} at the end of the day, (5) the energy level of each vehicle never drops below s^{min}, and (6) in each depot $k \in K$ at most b_k vehicles start and end their routes. We call such a schedule feasible. Among all feasible schedules the MDEVSP searches for the one which lexicographically minimizes (i) the number of used vehicles, (ii) the number of visits of charging stations, and (iii) the energy spent on deadhead trips. The latter is is equivalent to minimizing the total energy consumed since the energy spent on service trips is a constant value.

Bertossi et al. (1987) have shown that the vehicle scheduling problem with a single depot can be solved in polynomial time while its multi-depot version, the MDVSP, is NP-hard. Since the MDVSP is a special case of the MDEVSP, where the battery capacity of each vehicle $s^{max} = \infty$ and there are no charging stations, the MDEVSP is NP-hard as well.

Each feasible schedule represents the planned itinerary for all vehicles throughout the day. The schedule of one vehicle can be represented as an ordered sequence of service trips, depots and charging stations, so as an ordered sequence of elements from $V^I \cup O \cup D \cup C$. In particular, the first element of the sequence must belong to the set of origin depots O, the last to the set of destination depots D, and all others in between to $V^I \cup C$. Additionally, the sequence must include at least one service trip, no two consecutive charging stations can occur and each charging station can occur only directly after a service trip. This illustration of schedules as ordered sequences will be the foundation of our graph representation of the MDEVSP.

3.2 Graph representation

Our next step is to define a graph, such that each flow in this graph with certain properties corresponds to a feasible solution of the MDEVSP. To construct the graph, initially we set the set of nodes V as $V = V^I \cup V^D \cup V^C$, where the service trip node set V^I, the depot node set $V^D = O \cup D$, and the charging node set $V^C := \emptyset$ are used. Furthermore, we start with the arc set $A := \emptyset$. We add arcs to A and charging nodes to V^C by following these steps:

1. Generate arcs between depots and service trips: For each depot index $k \in K$, we generate an arc from the origin depot o_k to each service trip $i \in V^I$, as well as from each service trip $i \in V^I$ to the destination depot d_k.

2. Generate an arc between each pair of time-feasible service trips: For each pair of service trips $i, j \in V^I$, we create an arc if $s_i + u_i + t_{ij} \leq s_j$ holds.

3. Generate (and partially connect) full charging nodes representing fully charging after service trips: For each service trip $i \in V^I$ and each charging station $a \in C$ we create a

charging node $c_{ia}^{full} \in V^C$ representing the possibility of fully charging at charging station a after service trip i. This charging node $c = c_{ia}^{full}$ has location $\ell_c = \ell_a$, maximum available charging time $t_c = t^{max}$ and maximum amount that can be charged $h_c = rt_c$. Additionally, we connect i and c with an arc and this arc has energy usage $p_{ic} = p_{ia}$.

4. Generate charging nodes and connect (full) charging nodes representing charging between two service trips: For each pair of service trips $i, j \in V^I$, we identify the set $C_{ij} \subseteq C$ of all charging stations, which are reasonable for charging a vehicle between the service trips i and j. To be more precise, a charging station $a \in C$ is in C_{ij}, if there is no other charging station $a' \in C$ that dominates a. A charging station a' dominates a charging station a, if (1) a' is closer to the end location ℓ_i^e of service trip i than a and (2) a' is closer to the start location ℓ_j^s of service trip j than a (if such a charging station a' exists, then it would always be better to charge at a' than at a).

For each charging station $a \in C_{ij}$, we compute the maximum available charging time $t_{ija} = \min\{s_j - (s_i + u_i + t_{ia} + t_{aj}), t^{max}\}$ and the maximum amount that can be charged $h_{ija} = rt_{ija}$. If the energy required to travel from service trip i to service trip j via charging station a is less than the amount that can be recharged at charging station a, so if $p_{ia} + p_{aj} < h_{ija}$, we do the following case distinction.

On the one hand, if we can fully charge, so if $t_{ija} = t^{max}$, then we use the full charging node $c = c_{ia}^{full}$, we connect c and j with an arc and we set $p_{cj} = p_{aj}$.

On the other hand, if we can not fully charge, but we can charge at least t^{min} minutes, so if $t^{max} > t_{ija} \geq t^{min}$, then we generate a charging node $c_{ija}^{part} \in V^C$ representing charging at a between the service trips i and j. Charging node $c = c_{ija}^{part}$ has location $\ell_c = \ell_a$, maximum available charging time $t_c = t_{ija}$ and maximum amount that can be charged $h_c = h_{ija}$. Additionally, we connect both i and c and c and j with an arc and set the energy usage $p_{ic} = p_{ia}$ and $p_{cj} = p_{aj}$.

5. Generate arcs representing fully charging before returning to the depot: For each service trip $i \in V^I$ and each destination depot $d_k \in D$, we determine the set $C_{id_k} \subseteq C$ of all charging stations, which are reasonable for charging a vehicle between service trip i and going back to the depot d_k. In particular, a charging station $a \in C$ is in C_{id_k}, if there is no other charging station $a' \in C$ such that (1) a' is closer to the end location ℓ_i^e of service trip i than a and (2) a' is closer to the depot location ℓ_{d_k} of depot d_k than a (because if such a charging station a' exists, then it would always be better to charge at a' than at a). For each charging station $a \in C_{id_k}$, we then connect the full charging node $c = c_{ia}^{full} \in V^C$ and d_k with an arc and set the energy usage $p_{c,d_k} = p_{a,d_k}$.

This gives us the graph $G = (V, A)$. For illustration purposes, we provide a small example instance I_1. We consider three service trips $V^I = \{ST_1, ST_2, ST_3\}$, one depot (resulting in the start depot o_1 and the end depot d_1), and two charging stations $C = \{a_1, a_2\}$. Furthermore, we assume that the vehicles start fully charged from the depot.

t_{ij}	ST_1	ST_2	ST_3	o_1/d_1	o_2/d_2	a_1	a_2		s_i	e_i
ST_1	-	28	5	34	15	28	19	ST_1	01:15 p.m.	02:00 p.m.
ST_2	28	-	5	34	15	28	19	ST_2	04:30 p.m.	05:15 p.m.
ST_3	35	35	-	7	49	32	23	ST_3	05:05 p.m.	06:30 p.m.
o_1/d_1	40	40	29	-	47	26	26			
o_2/d_2	39	39	19	47	-	33	34			
a_1	50	50	24	20	30	-	36			
a_2	15	15	16	26	34	35	-			

Table 1: Traveling time t_{ij} between service trips, depots, and charging stations, as well as the service trips' start and end times s_i and e_i for the example graph in Figures 1 and 2.

The travel time t_{ij} between service trips, depots, and charging stations, as well as the start time s_i and end time e_i of each service trip can be found in Table 1. The time t^{max} it takes to fully charge a vehicle at a full charging node c_{ia}^{full} is set to 120 minutes. Recharging at the partial charging nodes c_{121}^{part} and c_{122}^{part} is possible for 72 and 116 minutes, respectively. However, since charging station a_2 is closer to ST_1 as well as to ST_2 than a_1, ST_1 and ST_2 are only connected via c_{122}^{part}. The same holds for ST_1 and ST_3, where enough time is available to fully recharge, but again a_2 is closer to both ST_1 and ST_3 than a_1. Therefore, ST_1 and ST_3 are only connected via c_{12}^{full}. An example of the graph for instance I_1 is provided in Figure 1.
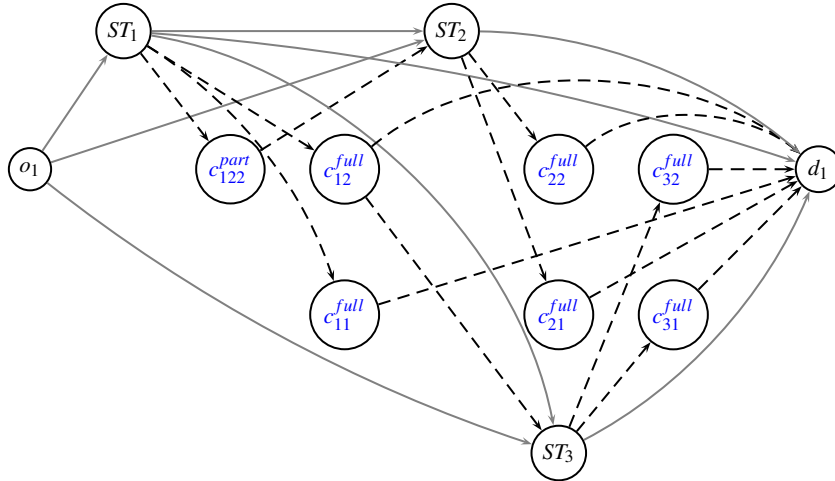
Figure 1: Graph for the instance I_1 with a single origin (o_1) and destination (d_1) depot.

Grey arcs are direct connections between service trips and between service trips and depots. Black dashed arcs connect service trips with charging nodes, as well as charging nodes with the depot. All connections are time feasible. E.g., ST_2 and ST_3 are not connected via an arc, since ST_2 ends at 5:15 p.m. but ST_3 already starts at 5:05 p.m. All service trips are connected via two full charging nodes to the end depot d_1, because charging station a_1 is closer to the depot while a_2 is closer to the service trips. Thus, connections via full charging nodes have been generated for all combinations of service trips and charging stations.

For another example instance I_2, which is identical to the instance I_1, except for the addition of an extra depot, we examine a small example of the corresponding graph provided in Figure 2. The service trips as well as the reasonable full charging nodes are now connected to both depots.

The rest of the graph structure remains unchanged from Figure 1.
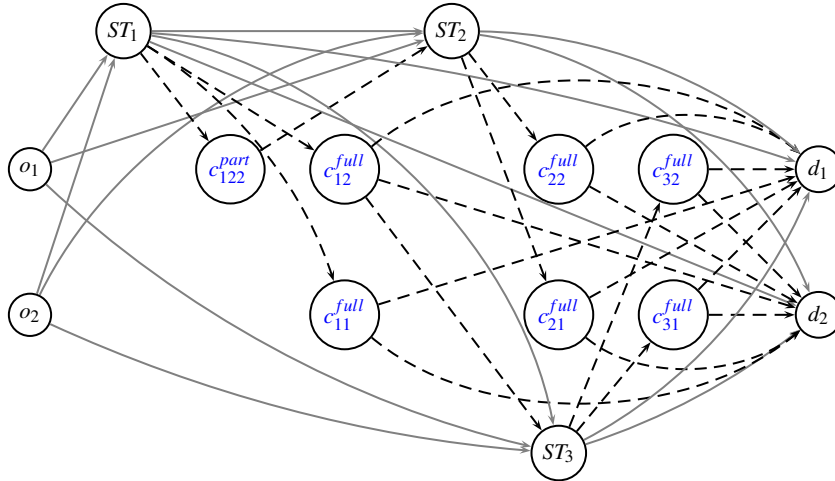
Figure 2: Graph for the instance I_2 with two origin depots (o_1, o_2) and two destination depots (d_1, d_2).

Eventually, we have defined the graph $G = (V, A)$ such that each feasible solution of the MDEVSP corresponds to a certain type of flow (namely one that makes sure that each unit of flow ends at the same depot as it starts) in G. In particular, in such a flow each unit of flow represents the schedule of one vehicle and starts from an origin depot $o_k \in O$ for some $k \in K$ and ends at the corresponding destination depot $d_k \in D$. Note that we have embedded all time relevant information into the graph construction directly, such that any flow in our graph will automatically correspond to a time feasible schedule for the MDEVSP.

4   Mathematical models for the MDEVSP

The graph representation of the MDEVSP will now be the foundation of two mixed-integer linear programming formulations of the MDEVSP. First, we present a 3-index formulation in Section 4.1. Then we detail how we can omit one of the indices and derive a 2-index formulation in Section 4.2. Furthermore, we present valid inequalities and possible extensions in Section 4.3. Finally, we describe how our formulations can be adapted to alternative zero emission technologies in Section 4.4.

4.1   A 3-index formulation

We now present our first mixed-integer linear programming formulation for the MDEVSP based on the graph $G = (V, A)$ derived in Section 3.2, which we refer to as 3-index formulation. Our models are inspired by Stumpe et al. (2021) and Frieß and Pferschy (2021).

For notational convenience, we will denote by $A^-(i)$ and $A^+(i)$ the set of all predecessor and successor nodes of a node $i \in V$ in G, respectively. So $A^-(i) = \{j \in V : (j, i) \in A\}$ and $A^+(i) = \{j \in V : (i, j) \in A\}$ holds.

We introduce two sets of decision variables for this 3-index formulation: For each $k \in K$ and each $(i, j) \in A$ let $x_{ij}^k \in \{0, 1\}$ be a binary variable, which is 1, if the arc (i, j) is used from

vehicles associated with depot k, 0 otherwise. Furthermore, for each $i \in V$, let ε_i be the energy level of vehicles when leaving node i. With these decision variables the 3-index MDEVSP can be formulated as the mixed-integer multi-commodity flow model

$$\min \ w_1\Big(\sum_{k \in K} \sum_{j \in A^+(o_k)} x_{o_k,j}^k\Big) + w_2\Big(\sum_{k \in K} \sum_{c \in V^C} \sum_{i \in A^-(c)} x_{ic}^k\Big) + \ w_3\Big(\sum_{k \in K} \sum_{(i,j) \in A} p_{ij} x_{ij}^k\Big) \tag{1a}$$

$$\text{s.t.} \ \sum_{k \in K} \sum_{i \in A^-(j)} x_{ij}^k = 1 \qquad\qquad\qquad \forall j \in V^I \tag{1b}$$

$$\sum_{j \in A^+(o_k)} x_{o_k,j}^k \leq b_k \qquad\qquad\qquad \forall k \in K \tag{1c}$$

$$\sum_{i \in A^-(j)} x_{ij}^k = \sum_{i \in A^+(j)} x_{ji}^k \qquad\qquad \forall j \in V \setminus V^D, k \in K \tag{1d}$$

$$\sum_{j \in A^+(o_k)} x_{o_k,j}^k = \sum_{i \in A^-(d_k)} x_{i,d_k}^k \qquad \forall k \in K \tag{1e}$$

$$\sum_{\substack{k' \in K \\ k' \neq k}} \sum_{j \in A^+(o_{k'})} x_{o_{k'},j}^k = 0 \qquad\qquad \forall k \in K \tag{1f}$$

$$\sum_{\substack{k' \in K \\ k' \neq k}} \sum_{i \in A^-(d_{k'})} x_{i,d_{k'}}^k = 0 \qquad\qquad \forall k \in K \tag{1g}$$

$$\varepsilon_{o_k} = s^{max} \qquad\qquad\qquad\qquad \forall k \in K \tag{1h}$$

$$s^{min} \leq \varepsilon_i \qquad\qquad\qquad\qquad \forall i \in V \setminus V^D \tag{1i}$$

$$s^{min}_{dep} \leq \varepsilon_{d_k} \qquad\qquad\qquad\qquad \forall k \in K \tag{1j}$$

$$s^{min} \leq \varepsilon_i - \sum_{j \in A^+(i)} p_{ij} x_{ij}^k \qquad\qquad \forall i \in V^I, k \in K \tag{1k}$$

$$\varepsilon_j \leq \varepsilon_i - (p_{ij} + q_j) x_{ij}^k + s^{max}(1 - x_{ij}^k) \quad \forall j \in V^I, i \in A^-(j), k \in K \tag{1l}$$

$$\varepsilon_c \leq \varepsilon_i - (p_{ic} - h_c) x_{ic}^k + s^{max}(1 - x_{ic}^k) \quad \forall c \in V^C, i \in A^-(c), k \in K \tag{1m}$$

$$\varepsilon_{d_k} \leq \varepsilon_i - p_{i,d_k} x_{i,d_k}^k + s^{max}(1 - x_{i,d_k}^k) \quad \forall k \in K, i \in A^-(d_k) \tag{1n}$$

$$\varepsilon_c \leq s^{max} \qquad\qquad\qquad\qquad \forall c \in V^C \tag{1o}$$

$$x_{ij}^k \in \{0,1\} \qquad\qquad\qquad\qquad \forall (i,j) \in A, k \in K. \tag{1p}$$

The objective function (1a) minimizes, in a lexicographic way, first the number of vehicles (which equals the number of used arcs leaving all origin depots o_k), second the number of charging events during the day (which equals the sum of the used arcs entering any of the charging nodes c), and third the energy spent on deadhead trips (which equals the required energy for all used arcs). Towards this end, the objective function uses the weights w_1, w_2, $w_3 \in \mathbb{R}$, which must be set appropriately and fulfill $w_1 > w_2 > w_3$.

Constraints (1b) make sure that each service trip node $j \in V^I$ is visited exactly once. Constraints (1c) limit the number of vehicles that can be used at each depot. Constraints (1d) ensure flow conservation (if a node is entered it has to be left unless it is a depot). Constraints (1e) make sure that at each depot the same number of vehicles leaves and arrives. Constraints (1f) guarantee that vehicles associated with the depot with index k use only arcs leaving origin depot

o_k and no arcs leaving another origin depot $o_{k'}$ for some $k' \neq k$, while constraints (1g) ensure that vehicles associated with the depot with index k use only arcs arriving at destination depot d_k and no arcs arriving at another destination depot $d_{k'}$ for some $k' \neq k$.

Constraints (1h) set the energy level at all origin depots to the maximum energy level (all vehicles leave the depots fully charged). Constraints (1i) make sure that the energy level when leaving any node except the depots is not below the minimum required energy level. Constraints (1j) ensure that the energy level when returning to the depot is not below the required energy level at the destination depot. Constraints (1k) make sure that the energy level is not below the minimum required energy level before arriving at the charging station (which is implied by the fact that the energy level is not below the minimum required energy level when arriving at the next node after a service trip node, as charging nodes are always preceded by service trip nodes). Constraints (1l) guarantee that the energy level at the end of a service trip corresponds to the energy level of the previous node minus the energy that was consumed by the deadhead trip connecting the previous node and this service trip and the energy used by the service trip itself. Constraints (1m) allow the energy level at the end of a charging node to rise to at most the energy level of the previous node minus the energy that was consumed by the deadhead trip connecting the previous node and the charging station plus the energy that can be loaded at this charging node. Constraints (1n) make sure that the energy level at the destination depots correspond to at most the energy level at the previous node minus the energy spent on the deadhead trip connecting the previous node to the depot. Constraints (1o) make sure that a vehicle cannot be charged to an energy level that is higher than the battery capacity. The domain of the variable x is defined in (1p).

Note, that (1) is a compact mixed-integer linear program, that can be solved with off-the-shelve solvers. We will present computational results for doing so later on.

4.2 A 2-index formulation

Next, we present a second mixed-integer linear programming formulation for the MDEVSP. Like our first formulation (1), it is based on the graph $G = (V, A)$ derived in Section 3.2.

For this new formulation, which we refer to as 2-index formulation, we introduce a binary decision variable $x_{ij} \in \{0, 1\}$ for each $(i, j) \in A$. It is 1 if arc (i, j) is used by any vehicle, 0 otherwise. The second set of decision variables ε_i is used in the same sense as in the 3-index formulation, i.e., it is the energy level of vehicles when leaving node i for each $i \in V$. Then the 2-index formulation of the MDEVSP is given as

$$\min \ w_1 \Big(\sum_{k \in K} \sum_{j \in A^+(o_k)} x_{o_k,j} \Big) + w_2 \Big(\sum_{c \in V^C} \sum_{i \in A^-(c)} x_{ic} \Big) + \qquad w_3 \Big(\sum_{(i,j) \in A} p_{ij} x_{ij} \Big) \qquad (2a)$$

$$\text{s.t.} \ \sum_{i \in A^-(j)} x_{ij} = 1 \qquad\qquad \forall j \in V^I \qquad (2b)$$

$$\sum_{j \in A^+(o_k)} x_{o_k,j} \leq b_k \qquad\qquad \forall k \in K \qquad (2c)$$

$$\sum_{i \in A^-(j)} x_{ij} = \sum_{i \in A^+(j)} x_{ji} \qquad \forall j \in V \setminus V^D \tag{2d}$$

$$\sum_{j \in A^+(o_k)} x_{o_k,j} = \sum_{i \in A^-(d_k)} x_{i,d_k} \qquad \forall k \in K \tag{2e}$$

$$\sum_{(i,j) \in P} x_{ij} \leq |P| - 1 \qquad \forall P \in \mathcal{P} \tag{2f}$$

$$\varepsilon_{o_k} = s^{max} \qquad \forall k \in K \tag{2g}$$

$$s^{min} \leq \varepsilon_i \qquad \forall i \in V \setminus V^D \tag{2h}$$

$$s^{min}_{dep} \leq \varepsilon_{d_k} \qquad \forall k \in K \tag{2i}$$

$$s^{min} \leq \varepsilon_i - \sum_{j \in A^+(i)} p_{ij} x_{ij} \qquad \forall i \in V^I \tag{2j}$$

$$\varepsilon_j \leq \varepsilon_i - (p_{ij} + q_j) x_{ij} + s^{max}(1 - x_{ij}) \qquad \forall j \in V^I, i \in A^-(j) \tag{2k}$$

$$\varepsilon_c \leq \varepsilon_i - (p_{ic} - h_c) x_{ic} + s^{max}(1 - x_{ic}) \qquad \forall c \in V^C, i \in A^-(c) \tag{2l}$$

$$\varepsilon_{d_k} \leq \varepsilon_i - p_{i,d_k} x_{i,d_k} + s^{max}(1 - x_{i,d_k}) \qquad \forall k \in K, i \in A^-(d_k) \tag{2m}$$

$$\varepsilon_c \leq s^{max} \qquad \forall c \in V^C \tag{2n}$$

$$x_{ij} \in \{0,1\} \qquad \forall (i,j) \in A, \tag{2o}$$

where $\mathcal{P}$ is the set of all paths $P = (v_1, ..., v_n)$ in G with $v_1, \ldots, v_n \in V$ and $(v_i, v_{i+1}) \in A$ for all $i = 1, \ldots, n-1$ from an origin depot $v_1 = o_k$ for some $k \in K$ to another other destination depot $v_n = d_{k'}$ for some $k' \in K \setminus \{k\}$. Thus, the so-called infeasible path constraints (2f) (see, e.g., Ascheuer et al., 2000) ensure that no vehicle takes an infeasible path (starting and ending in a different depot).

All other constraints of the 2-index formulation (2) are defined analogously to the constraints of the 3-index formulation (1), with the difference that now, we do not have a separate variable x_{ij}^k for each $k \in K$ representing vehicles associated to the depot $k \in K$, but only one variable x_{ij} for each arc $(i,j) \in A$. Thus, it is not possible to tell directly from the variables of (2) at which depot a vehicle using the arc (i,j) departed. This advantage of having fewer variables comes at the cost of having a high number of infeasible path constraints (2f). We describe in Section 5.1 how to deal with this computationally.

Another option to avoid the undesirable infeasible paths is by replacing constraints (2f) with other constraints similar to how it is done, e.g. in Parragh (2011). For doing so, for each $k \in K$ we introduce the set $\mathcal{U}_k$ of all node subsets $U \subseteq V$, such that the origin depot $o_k \in U$ and the destination depot $d_k \notin U$, while for all other $k' \in K \setminus \{k\}$ the origin depots $o_{k'} \notin U$ and the destination depots $d_{k'} \in U$. Then, we can replace the infeasible path constraints (2f) in the 2-index formulation (2) with

$$\sum_{i \in U} \sum_{j \in A^+(i), j \notin U} x_{ij} \geq \sum_{j \in A^+(o_k)} x_{o_k,j} \qquad \forall k \in K, U \in \mathcal{U}_k. \tag{3}$$

These connectivity constraints (3) ensure that for every $k \in K$ every vehicle leaving the origin depot o_k must exit the set U (which contains o_k) and enter the set $V \setminus U$ (which contains d_k),

guaranteeing the correct pairing of the corresponding depots. Note that the cardinality of each of the sets $\mathcal{U}_k$ is $2^{|V^I \cup V^C|}$, as $V = V^I \cup V^D \cup V^C$, so there are exponentially many connectivity constraints (3). We detail in Section 5.2 how we treat them in our computations.

4.3   Valid inequalities

We now turn our attention to improving the MILP models (1) and (2) by adding valid inequalities. Our first valid inequalities are based on a lower bound of vehicles needed for covering all the service trips. In particular, we determine the maximum number of concurrent service trips LB, which is defined as the maximum number of service trips that are timetabled at the same time. This count LB provides us with a lower bound on the required number of vehicles, i.e., the number of vehicles leaving any of the origin depots o_k. Thus,

$$\sum_{k \in K} \sum_{j \in A^+(o_k)} x_{o_k,j}^k \geq LB \tag{4a}$$

is a valid inequality for the 3-index formulation (1) and

$$\sum_{k \in K} \sum_{j \in A^+(o_k)} x_{o_k,j} \geq LB \tag{4b}$$

is a valid inequality for the 2-index formulation (2).

Our second set of valid inequalities for the 3-index formulation (1) is based on decreasing the constant of the big-M-type constraints (1l), (1m) and (1n) that ensure that the energy level of each vehicle is propagated through the graph in the right way. In particular, $\varepsilon_i \geq s^{min}$ is always fulfilled for each $i \in V$ because of (1h), (1i) and (1j). Thus, the constant s^{max} in the constraints (1l), (1m) and (1n) can be replaced by the smaller constant $(s^{max} - s^{min})$ and hence (1l), (1m) and (1n) can be strengthened to

$$\varepsilon_j \leq \varepsilon_i - (p_{ij} + q_j)x_{ij}^k + (s^{max} - s^{min})(1 - x_{ij}^k) \qquad \forall j \in V^I, i \in A^-(j), k \in K \tag{5a}$$

$$\varepsilon_c \leq \varepsilon_i - (p_{ic} - h_c)x_{ic}^k + (s^{max} - s^{min})(1 - x_{ic}^k) \qquad \forall c \in V^C, i \in A^-(c), k \in K \tag{5b}$$

$$\varepsilon_{d_k} \leq \varepsilon_i - p_{i,d_k}x_{i,d_k}^k + (s^{max} - s^{min})(1 - x_{i,d_k}^k) \qquad \forall k \in K, i \in A^-(d_k). \tag{5c}$$

With this smaller constant the same integer solutions remain feasible for the 3-index formulation (1), while the feasible region of the linear relaxation becomes smaller, leading to hopefully stronger LP bounds.

Analogously, one obtains valid inequalities for the 2-index formulation (2) by

$$\varepsilon_j \leq \varepsilon_i - (p_{ij} + q_j)x_{ij} + (s^{max} - s^{min})(1 - x_{ij}) \qquad \forall j \in V^I, i \in A^-(j) \tag{6a}$$

$$\varepsilon_c \leq \varepsilon_i - (p_{ic} - h_c)x_{ic} + (s^{max} - s^{min})(1 - x_{ic}) \qquad \forall c \in V^C, i \in A^-(c) \tag{6b}$$

$$\varepsilon_{d_k} \leq \varepsilon_i - p_{i,d_k}x_{i,d_k} + (s^{max} - s^{min})(1 - x_{i,d_k}) \qquad \forall k \in K, i \in A^-(d_k). \tag{6c}$$

4.4 Extension to alternative zero emission technologies

Finally, we want to point out that even though we have created the graph and derived the two MILP formulations (1) and (2) for the MDEVSP considering electric charging at dedicated charging stations, it is also possible to apply our framework for alternative zero emission technologies.

For example, our model is able to depict the possibility of opportunity charging at the start or end locations of the service trips. To do so, for each service trip $i \in V^I$, if opportunity charging is available at the start (end) location of the service trip ℓ_i^s (ℓ_i^e), then a charging station a is added to C at location $\ell_a = \ell_i^s$ ($\ell_a = \ell_i^e$) and the corresponding values of t_{ij}, d_{ij} and p_{ij} for $i = a$ or $j = a$ need to be adapted accordingly. Only then the graph is constructed.

Moreover, the option of overnight charging at a depot $k \in K$ can be integrated into the model by creating a charging station a at the location ℓ_k of the depot k.

Furthermore, fuel cell electric buses can be considered with our methodology if the charging stations $a \in C$ represent hydrogen fueling stations, and the energy consumption rate θ, the charging rate r, the maximum energy level s^{max}, the minimum energy level s^{min} and s_{dep}^{min} and the minimum time that needs to be available for charging t^{min} are modified to fit for the fuel cell case.

Thus, our approach is universal in the sense that it can be adapted to various zero emission technology settings. Also, the consideration of diesel buses is possible with our model analogously to the fuel cell case.

5 Branch-and-cut algorithm

In order to employ the previously introduced 3-index formulation (1) and 2-index formulation (2) for solving the MDEVSP, one could use one of many available MILP solvers in the standard configuration. While this is possible for (1), the large number of infeasible path constraints (2f) or connectivity constraints (3) becomes prohibitive for (2).

Thus, we have developed a branch-and-cut algorithm for (2). Branch-and-cut algorithms incorporate the principles of branch-and-bound and pair it with the cutting-plane idea. They start from solving the linear relaxation of the MILP, while considering only a reasonable subset of the original constraints. Typically, constraints of exponential size are excluded. Then, in the course of the algorithm a separation method is required, which finds violated constraints and adds them in an iterative fashion, until ultimately no original constraints are violated anymore, even though they might not be included explicitly.

In our branch-and-cut algorithm, we start with solving (2) with all constraints except for the infeasible path constraints (2f), which are initially omitted. We call this model the base model from now on. We now explore two options for the branch-and-cut algorithm: either we separate and add infeasible path constraints (2f), or connectivity constraints (3) in the course of our algorithm.

5.1 Separation of infeasible path constraints

We start by investigating the separation of infeasible path constraints (2f). Whenever we are given a feasible solution (x, ε) to the base model (which implies integrality of the variables x_{ij} for each arc $(i, j) \in A$ because of (2o)), we check if there is a path $P = (v_1, \ldots, v_n)$ in $G = (V, A)$ with $v_1, \ldots, v_n \in V$ and $(v_i, v_{i+1}) \in A$ such that $x_{v_i, v_{i+1}} = 1$ for all $i = 1, \ldots, n - 1$ that starts in a depot $v_1 = o_k$ for some $k \in K$ and ends in another depot $v_n = d_{k'}$ for some $k' \in K \setminus \{k\}$. Such a path P corresponds to a vehicle arriving at a different depot than it started and hence is infeasible, which implies that (x, ε) is feasible for the base model, but infeasible for the 2-index formulation (2). As a result, such an infeasible path must be prohibited.

Clearly, whenever one infeasible path is found, at least one other path is violated, as the number of vehicles departing and arriving at each depot is the same. Thus, we consider two different options: either we add only one infeasible path constraint (2f) as soon as we find the first infeasible path P (option `One`), or we collect all infeasible paths and add the constraint (2f) for all of them (option `All`).

In the so far described separation we only separate whenever an integer solution is encountered within the branch-and-cut algorithm. We will refer to this setting as `I`. It is possible to additionally use a separation in the case a fractional solution (i.e, a feasible solution to the linear relaxation of the current node problem in the branch-and-bound tree) is encountered. In particular, whenever we are given a feasible solution (x, ε) to the linear relaxation of the base model, we check if there is a path $P = (v_1, \ldots, v_n)$ in $G = (V, A)$ with $v_1, \ldots, v_n \in V$ and $(v_i, v_{i+1}) \in A$ such that $x_{v_i, v_{i+1}} > 0.00001$ for all $i = 1, \ldots, n - 1$ that starts in a depot $v_1 = o_k$ for some $k \in K$ and ends in another depot $v_n = d_{k'}$ for some $k' \in K \setminus \{k\}$, and such that the infeasible path constraint (2f) is violated for P. Whenever such an infeasible path is found, we add it in the same fashion as in setting `I`. We refer to this setting of separating for both integer and fractional solutions as `IF`. Note, that this kind of separation is optional in the sense that even though no fractional solutions are separated, the branch-and-cut algorithm is still correct, as only integer feasible solutions need to be separated for correctness.

5.2 Separation of connectivity constraints

Next, we draw our attention to separating the connectivity constraints (3). For a feasible solution (x, ε) to the base model (where x_{ij} is binary for each arc $(i, j) \in A$), we first check for a depot with index $k \in K$, whether there is an infeasible path starting in depot o_k and ending in a different depot $d_{k'}$ for some $k' \in K \setminus \{k\}$ like it is done in the separation for infeasible path constraints described in Section 5.1. If we have identified a depot with index $k \in K$ where an infeasible path starts, we want to identify a set $U \in \mathcal{U}_k$ for which the connectivity constraint (3) is violated by a large amount. To do so, we solve a max flow problem with source o_k and sink d_k in the graph $G = (V, A)$, where the capacity of an arc (i, j) is exactly the value of x_{ij}. This allows to determine a minimum cut $(T, V \setminus T)$ with $T \subseteq V$, $o_k \in T$ and $d_k \in V \setminus T$ by the

max-flow min-cut theorem such that

$$\sum_{i \in T} \sum_{j \in A^+(i), j \notin T} x_{ij} \tag{7}$$

is minimized, and thus $U = T$ can be used for adding a connectivity constraint (3). Note, that some technical modification is necessary for G in order to make sure that $o_{k'} \in V \setminus T$ and $d_{k'} \in T$ for all $k' \in K \setminus \{k\}$.

Again, due to the fact that if some path is infeasible, there are at least two depots $k \in K$ such that an infeasible path starts in k, we have the option of stopping the separation and adding the constraint as soon as one infeasible path is found (option `One`), or we can determine a set U for all depots $k \in K$ in which infeasible paths start and add a constraint (3) for all such depots (option `All`).

Additionally, we consider both the classical setting `I` of separating only integer solutions, and separating both integer and fractional solutions `IF` analogously as in the separation of infeasible path constraints. Again, both versions ensure correctness of our branch-and-cut algorithm.

6 Computational experiments

We are now able to present computational results. In the following, first, the attributes of the generated test instances are described in Section 6.1. Then, our obtained results are discussed for instances with a single depot in Section 6.2, a low number of depots (two, three, and four) in Section 6.3 and a high number of depots (six and eight) in Section 6.4.

6.1 Computational setup and test instances

Everything is implemented in Julia 1.11.1. For the branch-and-cut algorithms CPLEX 22.1 is employed, where for the separation as described in Section 5 we utilize `LazyConstraint` for separating integer solutions and `UserCut` for separating fractional solutions. In the separation of the connectivity constraints (3) described in Section 5.2 we use the Boykov-Kolmogorov algorithm within the function `maximum_flow()` of Julia in order to determine a minimum cut. All experiments were carried out on a Quad-core X5570 Xeon CPU @2.93GHz with a memory of 48 GB.

For our computational experiments, we use a set of MDEVSP benchmark instances generated in a similar way to the generation of MDVSP class A instances in Carpaneto et al. (1989) used by many other researchers (see Gkiotsalitis et al. (2023); Bianco et al. (1994); Fischetti et al. (2001); Forbes et al. (1994); Ribeiro and Soumis (1994)). The instances of Carpaneto et al. (1989) are not directly applicable to our setting, as they do not involve electric vehicles, which necessitate the inclusion of charging infrastructure in the instance data. Thus, we have created instances as close as possible to Carpaneto et al. (1989) and adapted them to the electric case as it was done in Gkiotsalitis et al. (2023).

In particular, we consider instances with $|V^I| \in \{10, 20, 30, 40, 50, 60\}$ service trips, $|K| = |O| = |D| \in \{1, 2, 3, 4, 6, 8\}$ depots, and $|C| \in \{1, 2, 3\}$ charging stations. For each instance, we

first determine a number ν of potential start and end locations of service trips (so-called relief locations) by choosing ν as uniformly random integer in $\left[\frac{1}{3}|V^I|, \frac{1}{2}|V^I|\right]$. Then we choose the ν relief locations $\ell_1^{ST}, \ldots, \ell_\nu^{ST}$, the depot locations ℓ_k for each $k \in K$, as well as the charging station locations ℓ_a for each $a \in C$ randomly distributed in a 60 km by 60 km square in the Euclidean plane using a uniform distribution, resulting in coordinates (latitude and longitude) for each location. Finally, for each service trip $i \in V^I$ we decide if it is a short trip (with probability 40%, representing urban journeys) or a long trip (with probability 60%, representing extra-urban journeys that start and end at the same location). Then for each service trip $i \in V^I$ we choose both the start and the end location of the service trip ℓ_i^s and ℓ_i^e uniformly at random as one of the ν relief locations $\ell_1^{ST}, \ldots, \ell_\nu^{ST}$, where we make sure that $\ell_i^s = \ell_i^e$ holds for long service trips i. From these locations we compute the distances d_{ij} as the Euclidean distances between the (end) location of i and the (start) location of j for each $i, j \in V^I \cup O \cup D \cup C$. For the travel times t_{ij} (in minutes) we assume an average vehicle speed of 60 km per hour translating to 1 km per minute, so $t_{ij} = d_{ij}$.

For each short service trip $i \in V^I$ we generate the start time s_i (in minutes since midnight) as a random integer in the interval $[420,480]$ with a probability of 15%, in the interval $[480,1020]$ with a probability of 70% and in the interval $[1020,1080]$ with a probability of 15%. Moreover, we choose the end time e_i uniformly at random as integer in the interval $[s_i + d_i + 5, s_i + d_i + 40]$, where d_i is the Euclidean distance between ℓ_i^s and ℓ_i^e. For each long service trip $i \in V^I$ we generate the start time s_i as a uniform random integer in the interval $[300,1200]$ and the end time e_i as a uniform random integer in the interval $[s_i + 180, s_i + 300]$. For each service trip $i \in V^I$ this yields the duration u_i, from which we compute the energy usage q_i as $q_i = \theta u_i$.

For each depot index $k \in K$ we generate the number of vehicles available as b_k as a uniformly random integer in $[3 + \frac{1}{3|K|}|V^I|, 3 + \frac{1}{2|K|}|V^I|]$. The parameters related to vehicles and charging are set to $\theta = 1.3$, $s^{max} = 1000$, $s^{min} = 10$ and $r = \frac{50}{6}$ as it is done in Gkiotsalitis et al. (2023). Note, that this yields $t^{max} = \frac{1}{r}(s^{max} - s^{min}) = 118.8$. Furthermore, we use $s_{dep}^{min} = 0.7 s^{max}$ and $t^{min} = \frac{1}{100} s^{max}$.

For each instance, we first generate the graph $G = (V, A)$ as described in Section 3.2. As this can be done quite fast (2.35 seconds for the largest instance) we omit the running time for doing so from now on. This yields graphs with a broad range of sizes, ranging from $|V| = 40$ and $|A| = 190$ for one of the smallest instances with $|V^I| = 10$, $|K| = 1$ and $|C| = 1$ up to $|V| = 917$ and $|A| = 9120$ for one of the largest instances with $|V^I| = 60$, $|K| = 8$ and $|C| = 3$. Note that the majority of the nodes of G is charging nodes ($|V^C| = 851$ for the latter instance with $|V| = 917$).

The graphs $G = (V, A)$ enable us to utilize the 3-index formulation (1) and the 2-index formulation (2) and its variant. For the weights of the objective functions of (1) and (2) we carefully engineered $w_1 = 100,000$, $w_2 = 4,000$ and $w_3 = 1$ as appropriate weights for all our instances, to make sure that we indeed minimize the desired quantities (number of vehicles, number of charging events, energy usage for deadhead trips) in lexicographic order.

6.2 Results for a single depot

We start by investigating instances with only one depot, so $|K| = |O| = |D| = 1$. For these instances the 3-index formulation (1) and the 2-index formulation (2) coincide, as neither infeasible path constraints (2f) (the set $\mathcal{P}$ is empty), nor connectivity constraints (3) (the set $\mathcal{U}_k$ is empty) are present.

We consider a set of 90 instances, namely five instances for each combination of $|V^I| \in \{10, 20, 30, 40, 50, 60\}$ service trips and $|C| \in \{1, 2, 3\}$ charging stations.

Table 2: Results for a single depot

$|V^I|$	$|C|$	#opt	t(s)	gap(%)	#nB&B	z^*	LB_R
10	1	10	0.05	0.00	22.6	471,689.05	469,066.54
10	2	10	0.07	0.00	3.2	471,093.91	469,758.28
10	3	10	0.30	0.00	0.0	552,536.49	551,906.75
20	1	10	0.11	0.00	178.4	864,496.71	862,890.77
20	2	10	0.24	0.00	217.4	843,637.16	841,021.47
20	3	10	0.68	0.00	864.0	760,955.41	756,186.32
30	1	10	1.54	0.00	1,910.1	1,112,737.81	1,100,675.44
30	2	10	0.95	0.00	879.0	1,154,218.11	1,146,477.21
30	3	10	3.02	0.00	1,624.5	1,155,001.82	1,141,261.63
40	1	10	6.53	0.00	5,111.9	1,466,963.22	1,450,335.05
40	2	10	321.87	0.00	209,772.8	1,486,804.98	1,467,894.73
40	3	8	2,167.82	0.30	846,177.5	1,464,963.46	1,444,291.56
50	1	10	70.63	0.00	35,872.8	1,613,935.37	1,572,182.94
50	2	9	2,497.99	0.21	942,411.9	1,734,256.53	1,693,949.86
50	3	8	2,174.41	0.94	743,048.8	1,654,094.08	1,624,816.48
60	1	8	4,388.87	0.19	1,327,319.6	2,043,139.67	1,998,699.10
60	2	8	2,164.61	0.20	365,917.0	2,208,161.83	2,167,048.28
60	3	8	4,062.17	0.44	944,193.8	1,962,828.15	1,932,322.04

In Table 2 we display results for a single depot. In particular, we present the number (#opt) of instances that were solved to optimality (out of 10), the average CPU times (t) in seconds, the average percentage gap at the time limit (3 hours) of all instances that were not solved to optimality, the average number of B&B nodes (#nB&B), the average best found objective function value z^* at termination and the average lower bound at the root node LB_R.

The results in Table 2 show that instances with a single-depot EVSP become more difficult with an increasing number of service trips, but not necessarily for an increasing number of charging stations, as the running times for the same number of service trips are sometimes higher with fewer charging stations. Furthermore, Table 2 shows that our formulation is able to solve nearly all single-depot instances with up to 40 service trips to proven optimality, and most of the instances with 50 and 60 service trips, demonstrating the effectiveness of the formulation for a single depot.

6.3 Results for a low number of depots

Next, we consider a set of 270 instances with two, three, and four depots, so $|K| = |O| = |D| \in \{2, 3, 4\}$. For each value of $|K|$ we investigate five instances for each combination of $|V^I| \in \{10, 20, 30, 40, 50, 60\}$ service trips and $|C| \in \{1, 2, 3\}$ charging stations.

Table 3: Results for all formulations for a low number of depots

setting			#opt	t(s)	gap(%)	#nB&B	z^*	LB_R	#cuts	t_{cut}(s)
3i+VI			176	3,824.48	0.620	431,497.1	1,254,985.23	1,229,348.96		
2i-IP+VI	I	One	191	3,463.46	0.530	567,248.1	1,252,516.59	1,226,759.39	632.23	6.14
	I	All	202	2,860.34	0.451	538,242.6	1,254,628.51	1,228,940.49	382.85	1.27
	IF	One	193	3,498.09	0.582	197,146.9	1,255,224.46	1,229,290.50	157,296.92	1,236.79
	IF	All	189	3,499.67	0.589	179,160.5	1,255,218.01	1,229,209.67	454,343.61	1,354.13
2i-CC+VI	I	One	194	3,406.85	0.518	490,587.1	1,255,123.02	1,229,223.12	379.12	6.70
	I	All	198	3,206.57	0.537	438,556.6	1,255,092.29	1,229,179.49	262.35	4.27
	IF	One	137	5,594.86	10.158	5,604.3	1,240,238.23	1,229,220.04	35,474.35	293.37
	IF	All	142	5,376.71	9.888	6,043.3	1,237,369.33	1,229,213.33	31,963.85	221.43

In Table 3 we display average results over all 270 instances for each available setting, namely for using

- the 3-index formulation (1) (named `3i`) with (`VI`) valid inequalities (4a), (5a), (5b) and (5c),

- the 2-index formulation (2), which includes the infeasible path constraints (2f) (named `2i-IP`), with separating only integer (`I`) or both integer and fractional (`IF`) solutions, with including all (`All`) or only the first (`One`) infeasible path constraint, with (`VI`) valid inequalities (4b), (6a), (6b) and (6c), and

- the 2-index formulation (2) without (2f) but with the connectivity constraints (3) (named `2i-CC`), with separating only integer (`I`) or both integer and fractional (`IF`) solutions, with including all (`All`) or only the first (`One`) connectivity constraint, and with (`VI`) valid inequalities (4b), (6a), (6b) and (6c).

For each of these settings, we give the number (#opt) of instances that were solved to optimality (out of 270), the average CPU times (t) in seconds, the average percentage gap at the time limit (3 hours) of all instances that were not solved to optimality, the average number of B&B nodes (#nB&B), the average best found objective function value z^* at termination, the average lower bound at the root node LB_R, the average number of cuts (i.e., added infeasible path constraints (2f) or added connectivity constraints (3)) and the average CPU time t_{cut} in seconds for the separation. For instances where no feasible solution was found within the time limit, we assume a gap of 100% and exclude z^* from the calculations.

The results in Table 3 clearly show that for `2i-CC+VI` all versions with separating fractional and integer solutions `IF` perform much worse and solve much fewer instances to optimality within the time limit, demonstrating the superiority of `I` for `2i-CC+VI`.

For `2i-IP+VI` the picture is not that clear, as in the setting `One`, `IF` performs slightly better than `I` with two more solved instances (193 vs. 191), while in the setting `All`, `IF` solves less instances than `I` (189 vs. 202).

Furthermore, the 2-index formulation with infeasible path constraints (`2i-IP+VI`) and both `I` and `IF` separations outperform the 3-index model in all settings (at least 189 instances are solved to optimality in all `2i-IP+VI` settings, while 176 instances are solved to optimality in `3i+VI`). Overall, the best setting of this computational evaluation is `2i-IP+VI+I+All` with 202 instances solved to optimality.

6.4 Results for a high number of depots

Finally, we consider a set of instances with $|K| = |O| = |D| \in \{6, 8\}$ depots. Here we consider for each value of $|K|$ five instances with $|C| = \{3, 4, 6\}$ charging stations for each number of service trips $|V^I| \in \{30, 40, 50, 60, 70, 80\}$, resulting in 180 instances in total.

Table 4: Results for 2-index formulations for a high number of depots

		#opt	t(s)	gap(%)	#nB&B	z^*	LB_R	#cuts	t_{cut}(s)
`2i-IP+VI+I`	`One`	44	7,730.64	51.28	591,526.70	1,532,739.78	1,736,747.63	6,899.24	102.15
`2i-IP+VI+I`	`All`	80	6,123.33	0.60	670,666.60	1,776,004.59	1,740,636.52	3,483.97	21.45
`2i-CC+VI+I`	`One`	52	6,883.98	23.58	420,146.80	1,684,375.49	1,737,303.19	2,653.12	108.58
`2i-CC+VI+I`	`All`	55	7,135.10	8.61	398,538.90	1,749,854.24	1,738,969.85	1,593.65	36.80

Table 4 gives the average results obtained with the 2-index model (2) in the two versions `2i-IF` and `2i-CC`, adding either all cuts (`All`) or only one (`One`) in each call of the separation routine. They are only separated on integer solutions (setting `I` from above) and the valid inequalities are active (setting `VI` from above). The columns of Table 4 are defined analogously to the columns of Table 2 and Table 3.

The settings `2i-IP+VI+I` and `2i-CC+VI+I` in combination with adding `All` cuts solve 80 and 55 instances out of 180 to optimality, respectively, and clearly outperform both settings with `One`. When comparing computation times, `2i-IP+VI+I+All` requires 6,123.33 seconds on average and solves 80 instances to optimality, while `2i-CC+VI+I+All` requires 7,135.10 seconds on average and solves 55 instances to optimality, indicating that `2i-IP+VI+I+All` has a clear edge over `2i-CC`. Overall, not only the number of optimally solved instances, but also the optimality gap is much better for both settings with `All` cuts added. In the end, the setting `2i-IP+VI+I+All` can be determined as clear winner in these runs.

In Table 5, we compare the best performing 2-index-based B&C algorithm `2i-IP+VI+I+All` with solving the 3-index formulation with valid inequalities with CPLEX directly for all 180 instances in detail, differentiating between the number of service trips $|V^I|$ and the number of depots $|K|$. For both the 2- and the 3-index formulation we present the number (#opt) of instances that were solved to optimality (out of 15), the average percentage gap at the time limit (3 hours) of all instances that were not solved to optimality and the average CPU times (t) in seconds.

In Table 5, we see that the 2-index formulation demonstrates superior overall performance in terms of number of instances solved to optimality (80 vs. 41). Furthermore, across all instance classes, the 2-index formulation consistently achieves significantly lower average optimality gaps and it generally requires notably less computational time, demonstrating the efficiency of our 2-index approach.

Table 5: Detailed results of 2-index and 3-index formulation for a high number of depots

		2-index (`2i-IP+VI+I+All`)			3-index (`3i+VI`)		
$|V^I|$	$|K|$	#opt	gap(%)	t(s)	#opt	gap(%)	t(s)
30	6	14	0.32	1,915.68	11	0.58	3,605.33
30	8	15	0.00	21.43	14	0.88	1,246.07
40	6	12	0.54	3,241.20	7	0.63	6,151.67
40	8	15	0.00	895.09	6	0.57	6,307.18
50	6	5	0.45	7,779.66	1	0.80	10,051.77
50	8	10	0.46	4,441.73	2	0.84	9,292.28
60	6	2	0.39	10,210.79	0	1.38	10,804.36
60	8	3	0.52	9,860.92	0	1.42	10,826.87
70	6	1	0.49	10,806.17	0	1.88	10,807.44
70	8	1	0.69	10,362.42	0	2.02	10,808.52
80	6	0	0.87	10,820.71	0	2.35	10,821.09
80	8	2	0.85	9,709.50	0	2.16	10,815.70

7 Conclusion

In this work, we have modeled and solved the electric vehicle scheduling problem with multiple depots, multiple charging stations and partial recharge. We have developed a graph representation that is an acyclic network and allows only time-feasible paths. Only two additional aspects need to be ensured for each vehicle schedule: the state-of-charge of the vehicles along a path, ensuring that vehicles cannot run out of energy, and that each vehicle returns to the same depot as it started from.

While our 3-index MILP can be solved with any off-the-shelf solver directly, in order to accommodate multiple depots, constraints of exponential size are incorporated into our 2-index MILP formulation. We compare two types of these constraints and different tailored separation strategies. The best performing strategy relies on infeasible path constraints, separated only at new integer incumbent solutions during the execution of the branch-and-cut algorithm. The 2-index-based branch-and-cut algorithm consistently solves more instances to optimality and in lower computation times than the 3-index model solved by CPLEX, for a low number of depots as well as for six and eight depots. Our approaches have been developed within the collaborative research project ZEMoS (Zero Emission Mobility Salzburg) and serve as decision support for fleet sizing decisions in two pilot regions in the country of Salzburg.

Future work will involve the development of heuristic approaches for more complex problem versions, such as heterogeneous vehicle fleets.

Acknowledgments

References

Adler, J. D. and Mirchandani, P. B. (2017). The vehicle scheduling problem for fleets with alternative-fuel vehicles. *Transportation Science*, 51(2):441–456.

Ascheuer, N., Fischetti, M., and Grötschel, M. (2000). A polyhedral study of the asymmetric traveling salesman problem with time windows. *Networks*, 36(2):69–79.

Bertossi, A. A., Carraresi, P., and Gallo, G. (1987). On some matching problems arising in vehicle scheduling models. *Networks*, 17(3):271–281.

Bianco, L., Mingozzi, A., and Ricciardelli, S. (1994). A set partitioning approach to the multiple depot vehicle scheduling problem. *Optimization Methods and Software*, 3(1-3):163–194.

BMK (2021). Austria's 2030 mobility master plan. `https://www.bmk.gv.at/en/topics/mobility/mobilitymasterplan2030.html` (accessed Jan 28, 2025).

Carpaneto, G., Dell'amico, M., Fischetti, M., and Toth, P. (1989). A branch and bound algorithm for the multiple depot vehicle scheduling problem. *Networks*, 19(5):531–548.

de Vos, M. H., van Lieshout, R. N., and Dollevoet, T. (2024). Electric vehicle scheduling in public transit with capacitated charging stations. *Transportation Science*, 58(2):279–294.

Diefenbach, H., Emde, S., and Glock, C. H. (2022). Multi-depot electric vehicle scheduling in in-plant production logistics considering non-linear charging models. *European Journal of Operational Research*.

EU (2019). Clean vehicles directive. `https://transport.ec.europa.eu/transport-themes/clean-transport/clean-and-energy-efficient-vehicles/clean-vehicles-directive_en` (accessed Jan 28, 2025).

Fischetti, M., Lodi, A., Martello, S., and Toth, P. (2001). A polyhedral approach to simplified crew scheduling and vehicle scheduling problems. *Management Science*, 47(6):833–850.

Forbes, M., Holt, J., and Watts, A. (1994). An exact algorithm for multiple depot bus scheduling. *European Journal of Operational Research*, 72(1):115–124.

Frieß, N. M. and Pferschy, U. (2024). Planning a zero-emission mixed-fleet public bus system with minimal life cycle cost. *Public Transport*, 16(1):39–79.

Frieß, N. and Pferschy, U. (2021). Decision-support system for the optimal technology split of a decarbonized bus network. In *2021 IEEE 45th Annual Computers, Software, and Applications Conference (COMPSAC)*.

Gerbaux, J., Desaulniers, G., and Cappart, Q. (2025). A machine-learning-based column generation heuristic for electric bus scheduling. *Computers & Operations Research*, 173:106848.

Gkiotsalitis, K., Iliopoulou, C., and Kepaptsoglou, K. (2023). An exact approach for the multi-depot electric bus scheduling problem with time windows. *European Journal of Operational Research*, 306(1):189–206.

Haslinger, X., Gaar, E., Parragh, S., Krisch, P., Schöpflin, F., and Prinz, T. (2023). Busflotteneinsatzplanung für den Umstieg auf batterieelektrische und H2-Brennstoffzellen-Busse im Raum Salzburg. In Brunner, U., Prandtstetter, M., Reiner, G., Starkl, F. P., Stein, S., and Walkolbinger, T., editors, *Jahrbuch der Logistikforschung*, volume 4, pages 75–86. Trauner Verlag + Buchservice GmbH.

Hu, H., Du, B., Liu, W., and Perez, P. (2022). A joint optimisation model for charger locating and electric bus charging scheduling considering opportunity fast charging and uncertainties. *Transportation Research Part C: Emerging Technologies*, 141:103732.

Janovec, M. and Koháni, M. (2019). Exact approach to the electric bus fleet scheduling. *Transportation Research Procedia*, 40:1380–1387.

Jiang, M. and Zhang, Y. (2022). A branch-and-price algorithm for large-scale multidepot electric bus scheduling. *IEEE Transactions on Intelligent Transportation Systems*, 24(12):15355–15368.

Li, J.-Q. (2014). Transit bus scheduling with limited energy. *Transportation Science*, 48(4):521–539.

Li, X., Wang, T., Li, L., Feng, F., Wang, W., and Cheng, C. (2020). Joint optimization of regular charging electric bus transit network schedule and stationary charger deployment considering partial charging policy and time-of-use electricity prices. *Journal of Advanced Transportation*, 2020:1–16.

Liu, T. and Ceder, A. A. (2020). Battery-electric transit vehicle scheduling with optimal number of stationary chargers. *Transportation Research Part C: Emerging Technologies*, 114:118–139.

Löbel, F., Borndörfer, R., and Weider, S. (2024). Electric bus scheduling with non-linear charging, power grid bottlenecks, and dynamic recharge rates. *arXiv preprint arXiv:2407.14446*.

Parragh, S. N. (2011). Introducing heterogeneous users and vehicles into models and algorithms for the dial-a-ride problem. *Transportation Research Part C: Emerging Technologies*, 19(5):912–930.

Perumal, S. S., Lusby, R. M., and Larsen, J. (2022). Electric bus planning & scheduling: A review of related problems and methodologies. *European Journal of Operational Research*, 301(2):395–413.

Peters, L., Dum, S., Riedl, H., Kainz, C., Nia, N. S., Fleischhacker, N., ohannes Mütterlein, Sagmeister, M., Kopp, K.-H., IskandarnZeynalov, Parragh, S., Haslinger, X., Gaar, E., Prinz, T., Krisch, P., Müller, C., Goers, S., Knöbl, M., Prieler, M., Wulff-Gegenbaur, J., Macho, H., and

Kerbl, G. (2024). Advancing sustainable transportation: Zero Emission Mobility Salzburg. In *Proceedings of the 18. Symposium Energieinnovation, 14.-16.02.2024, Graz/Austria*.

Ribeiro, C. C. and Soumis, F. (1994). A column generation approach to the multiple-depot vehicle scheduling problem. *Operations Research*, 42(1):41–52.

Rinaldi, M., Picarelli, E., D'Ariano, A., and Viti, F. (2020). Mixed-fleet single-terminal bus scheduling problem: Modelling, solution scheme and potential applications. *Omega*, 96:102070.

Sassi, O. and Oulamara, A. (2017). Electric vehicle scheduling and optimal charging problem: complexity, exact and heuristic approaches. *International Journal of Production Research*, 55(2):519–535.

Statista (2024a). Global distribution of CO_2 emissions 2023, by sector. `https://www.statista.com/statistics/1129656/global-share-of-co2-emissions-from-fossil-fuel-and-cement/` (accessed Jan 28, 2025).

Statista (2024b). Global transportation sector CO_2 emissions 1970-2023. `https://www.statista.com/statistics/1291615/carbon-dioxide-emissions-transport-sector-worldwide` (accessed Jan 28, 2025).

Stumpe, M. (2024). A new mathematical formulation for the simultaneous optimization of charging infrastructure and vehicle schedules for electric bus systems. *Transportation Research Procedia*, 78:402–409. 25th Euro Working Group on Transportation Meeting.

Stumpe, M., Rößler, D., Schryen, G., and Kliewer, N. (2021). Study on sensitivity of electric bus systems under simultaneous optimization of charging infrastructure and vehicle schedules. *EURO Journal on Transportation and Logistics*, 10:100049.

van Kooten Niekerk, M. E., Van den Akker, J., and Hoogeveen, J. (2017). Scheduling electric vehicles. *Public Transport*, 9:155–176.

Wang, C., Guo, C., and Zuo, X. (2021). Solving multi-depot electric vehicle scheduling problem by column generation and genetic algorithm. *Applied Soft Computing*, 112:107774.

Wen, M., Linde, E., Ropke, S., Mirchandani, P., and Larsen, A. (2016). An adaptive large neighborhood search heuristic for the electric vehicle scheduling problem. *Computers & Operations Research*, 76:73–83.

Wu, W., Lin, Y., Liu, R., and Jin, W. (2022). The multi-depot electric vehicle scheduling problem with power grid characteristics. *Transportation Research Part B: Methodological*, 155:322–347.

Yıldırım, Ş. and Yıldız, B. (2021). Electric bus fleet composition and scheduling. *Transportation Research Part C: Emerging Technologies*, 129:103197.

ZEMoS (2023). Zero emission mobility project webpage. https://www.wiva.at/project/zemos/ (accessed Jan 28, 2025).

Zhang, A., Li, T., Zheng, Y., Li, X., Abdullah, M. G., and Dong, C. (2022). Mixed electric bus fleet scheduling problem with partial mixed-route and partial recharging. *International Journal of Sustainable Transportation*, 16(1):73–83.

Zhang, L., Wang, S., and Qu, X. (2021). Optimal electric bus fleet scheduling considering battery degradation and non-linear charging profile. *Transportation Research Part E: Logistics and Transportation Review*, 154:102445.

Zhou, Y., Meng, Q., and Ong, G. P. (2022). Electric bus charging scheduling for a single public transport route considering nonlinear charging profile and battery degradation effect. *Transportation Research Part B: Methodological*, 159:49–75.

Zhou, Y., Meng, Q., Ong, G. P., and Wang, H. (2024). Electric bus charging scheduling on a bus network. *Transportation Research Part C: Emerging Technologies*, 161:104553.